

Polarization entanglement purification of nonlocal microwave photons based on the cross-Kerr effect in circuit QED*

Hao Zhang^{1,2}, Qian Liu³, Xu-Sheng Xu⁴, Jun Xiong¹, Ahmed Alsaedi², Tasawar Hayat^{2,5}, and Fu-Guo Deng^{1,2†}

¹*Department of Physics, Applied Optics Beijing Area Major Laboratory,
Beijing Normal University, Beijing 100875, China*

²*NAAM Research Group, Department of Mathematics,
King Abdulaziz University, Jeddah 21589, Saudi Arabia*

³*School of Sciences, Qingdao University of Technology, Qingdao 266033, China*

⁴*State Key Laboratory of Low-Dimensional Quantum Physics and
Department of Physics, Tsinghua University, Beijing 100084, China*

⁵*Department of Mathematics, Quaid-I-Azam University, Islamabad 44000, Pakistan*

(Dated: March 13, 2022)

Microwave photons have become very important qubits in quantum communication as the first quantum satellite has been launched successfully. Therefore, it is a necessary and meaningful task for ensuring the high security and efficiency of microwave-based quantum communication in practice. Here, we present an original polarization entanglement purification protocol for nonlocal microwave photons based on the cross-Kerr effect in circuit quantum electrodynamics (QED). Our protocol can solve the problem that the purity of maximally entangled states used for constructing quantum channels will decrease due to decoherence from environment noise. This task is accomplished by means of the polarization parity-check quantum nondemolition (QND) detector, the bit-flipping operation, and the linear microwave elements. The QND detector is composed of several cross-Kerr effect systems which can be realized by coupling two superconducting transmission line resonators to a superconducting molecule with the N -type level structure. We give the applicable experimental parameters of QND measurement system in circuit QED and analyze the fidelities. Our protocol has good applications in long-distance quantum communication assisted by microwave photons in the future, such as satellite quantum communication.

PACS numbers: 03.67.Pp, 85.25.Dq, 42.50.Pq, 03.67.Hk

I. INTRODUCTION

Quantum entanglement is an indispensable resource for quantum communication, such as quantum teleportation [1], quantum dense coding [2, 3], quantum key distribution [4–6], quantum secret sharing [7], and quantum secure direct communication [8–11]. To accomplish the quantum communication efficiently, the two legitimate remote parties usually use the photon pairs in maximally entangled states to construct their communication channel. Due to the decoherence from the environment in practice, the maximally entangled state will become a partially entangled state or a mixed entangled one. This consequence inevitably reduces the efficiency of the whole communication process. Therefore, some interesting methods are proposed to improve the efficiency of quantum communication, such as the error-rejecting coding with decoherence-free subspaces [12–14], entanglement concentration [15–19], and entanglement purification [20–34].

Entanglement purification is used to transfer a non-local mixed entangled state to a higher purity entangled state. It is a key technique in quantum repeaters for long-distance quantum communication to depress the harmful

influence of noise. To date, some interesting entanglement purification protocols (EPPs) have been proposed [20–34]. For example, in 1996, Bennett *et al.* [20] proposed an original EPP for photon pairs in a Werner state [35] by using two controlled-NOT gates and single-photon measurements. In 2001, Pan *et al.* [22] presented an EPP for a general mixed entangled state for an ideal entanglement source with simple linear optical elements. In 2002, Simon and Pan [23] proposed an EPP for a nonideal spontaneous parametric down conversion (PDC) source assisted by using spatial entanglement. In 2003, Pan *et al.* [24] demonstrated this EPP by using linear optical elements. In 2008, Sheng *et al.* [25] proposed an efficient polarization EPP for a PDC source based on the cross-Kerr effect. In 2010, Sheng and Deng [26] introduced the original EPP for two-photon systems in a deterministic way. In 2014, Ren and Deng [30] proposed a two-step hyperentanglement purification protocol (hyper-EPP) for two-photon four-qubit systems in nonlocal polarization-spatial hyperentangled Bell states. In 2016, Wang, Liu, and Deng [31] presented a universal method for hyper-EPP in the polarization degree of freedom and multiple-longitudinal-momentum degrees of freedom with SWAP gates.

Circuit quantum electrodynamics (QED), which couples the superconducting qubit to superconducting transmission line resonators (TLRs), provides a way to study the fundamental interaction between light and matter [36, 37]. It holds a big advantage on good scalability for

*Published in Phys. Rev. A **96**, 052330 (2017).

†Corresponding author: fgdeng@bnu.edu.cn

quantum information processing [38–46]. Many studies have focused on circuit QED [47–53]. As a very important and interesting phenomenon, the cross-Kerr effect has been researched in circuit QED in recent years [54–59]. For example, in 2009, Rebić *et al.* [54] proposed the giant Kerr nonlinearities at microwave frequencies in circuit QED. In 2011, Hu *et al.* [56] presented a theoretical scheme to generate the cross-Kerr effect between two TLRs. In 2013, Hoi *et al.* [58] observed the giant cross-Kerr effect for propagating microwaves experimentally induced by an artificial atom. In 2015, Holland *et al.* [59] demonstrated the single-photon resolved cross-Kerr effect between two microwave resonators in experiment. A microwave photon is a very important qubit for quantum communication because of its low loss and strong anti-interference during transmission. Due to the decoherence from environment, the maximally entangled microwave photon state may become a partially entangled pure state or a mixed one in the process of transmission and storage. To keep the high efficiency and fidelity of quantum communication, the legitimate parties in quantum communication should make an entanglement concentration or purification on the partially entangled microwave photon state or the mixed one, respectively. An original entanglement concentration protocol has been proposed for microwave photons [19]. To date, there is no research on entanglement purification of the nonlocal entangled states of microwave-photon pairs. Therefore, the entanglement purification of microwave-photon states is an extremely important and necessary task for microwave-based quantum communication. The microwave photon qubit can be manipulated effectively [53, 60, 61]. For example, Narla *et al.* [53] realized the basic microwave beam splitter which plays a very important role for microwave homodyne detection and used it to generate the robust concurrent remote entanglement between two superconducting qubits. The polarization can be manipulated by adjusting the material parameters [60, 61].

In this paper, we propose a physically feasible polarization EPP on the nonlocal entangled microwave photons in circuit QED. By using our EPP, the parties can effectively purify the mixed entangled states induced by the decoherence from environment noise in microwave-based quantum communication. This task is achieved with the polarization parity-check QND measurements on microwave-photon pairs, the bit-flipping operations, and the linear microwave elements. The parity-check quantum nondemolition (QND) detector is composed of two cross-Kerr systems for microwave photons and is a crucial part to implement the polarization entanglement purification. We give the applicable experimental parameters of a QND measurement system and analyze the fidelities. The protocol has some good applications in nonlocal microwave-based quantum communication, such as satellite quantum communication.

This article is organized as follows: We first review the cross-Kerr effect in circuit QED in Sec. II A and

then describe the process for the QND measurement on two cascade TLRs in Sec. II B. We present an EPP for microwave-photon pairs in Sec. III A and perform the EPP for polarization-spatial entangled microwave-photon pairs in Sec. III B. In Sec. III C, we design the reasonable parameters for QND measurement systems and analyze the fidelities. A summary is given in Sec. IV.

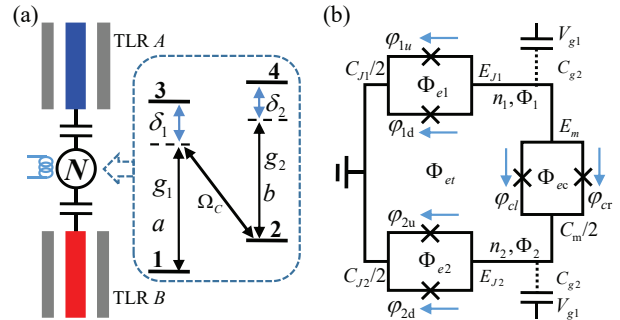


FIG. 1: (a) Schematic diagram of the cross-Kerr effect induced by coupling TLR A (top, blue) and B (bottom, red) to a superconducting molecule (middle, circle with N). The molecule can be controlled by external coils (left coils). The N -type level structure of the artificial molecule is shown in the right dashed line box. (b) The structure of superconducting quantum circuit for the molecule [56].

II. THE QND MEASUREMENT SYSTEM IN CIRCUIT QED

A. Cross-Kerr effect between two TLRs

The schematic diagram for realizing the cross-Kerr effect between two TLRs is shown in Fig. 1. The cross-Kerr effect can be realized by coupling two TLRs to a four level N -type superconducting molecule as shown in Fig. 1(a). The level structure is depicted in the dashed line box. TLR A and TLR B are coupled to the levels 1–3 and 2–4, respectively. The transition between the levels 2 and 3 is driven by a classical pump laser with the strength Ω_c . In the interaction picture, the Hamiltonian of the whole interaction system is given by [56] (with $\hbar = 1$)

$$\hat{H} = \delta_1 \hat{\sigma}_{33} + \delta_2 \hat{\sigma}_{44} + ig_1 (\hat{\sigma}_{13} \hat{a}^\dagger - \hat{\sigma}_{31} \hat{a}) + ig_2 (\hat{\sigma}_{24} \hat{b}^\dagger - \hat{\sigma}_{42} \hat{b}) + i\Omega_c (\hat{\sigma}_{23} - \hat{\sigma}_{32}), \quad (1)$$

where the detunings are $\delta_1 = E_{31} - \omega_1$ and $\delta_2 = E_{42} - \omega_2$. ω_1 and ω_2 are the frequencies of the TLRs A and B, respectively. $\hat{\sigma}_{ij} = |i\rangle\langle j|$ is the transition operator from the states $|j\rangle$ to $|i\rangle$. \hat{a} (\hat{a}^\dagger) and \hat{b} (\hat{b}^\dagger) are the annihilation (creation) operators for the modes of TLRs A and B, respectively. g_1 and g_2 are the coupling strengths for corresponding interactions between TLRs and levels.

Under the conditions that $|g_1/\Omega_c|^2 \ll 1$ and $|g_2| \ll |\delta_2|$ [64], one can adiabatically eliminate the atomic degrees of freedom and obtain the effective cross-Kerr interaction Hamiltonian [56]

$$\hat{H}_K = \chi \hat{a}^\dagger \hat{a} \hat{b}^\dagger \hat{b}, \quad (2)$$

where $\chi = -g_1^2 g_2^2 / (\delta_2 \Omega_c^2)$ is the cross-Kerr coefficient.

The molecule with an N -type level structure can be constructed in the superconducting circuit described in Fig. 1(b). The two loops (bottom and top) are two transmon qubits [62]. The right loop is a superconducting quantum interference device (SQUID) [63] which is used to connect two transmon qubits. Each loop is composed of two identical Josephson junctions labeled with crosses. $C_j/2$ ($j = m, 1, 2$) and E_{J_i} ($i = c, 1, 2$) represent the capacitance and energy of the Josephson junctions, respectively. The gate voltages labeled with V_{g1} and V_{g2} bias the corresponding transmons via the gate capacitors C_{g1} and C_{g2} , respectively. Φ_{e1} , Φ_{e2} , Φ_{ec} , and Φ_{et} are external fluxes. φ_{cr} , φ_{cl} , φ_{1u} , φ_{1d} , φ_{2u} , and φ_{2d} are the gauge-invariant phases across the Josephson junctions. By using the two-level language in the region $E_J \gg E_c$, one can obtain the N -type level form [56, 62] shown in Fig. 1(a). The eigenstates and the corresponding eigenvalues are $|i\rangle$ and E_i ($i = 1, 2, 3, 4$), respectively.

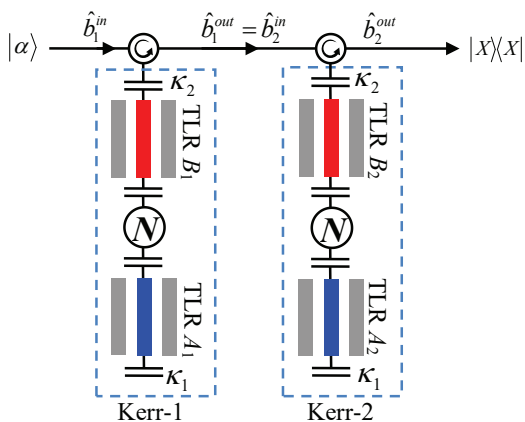


FIG. 2: Schematic diagram of QND measurement of the total photon number of the two TLRs labeled with A (i.e., A_1 and A_2). The two TLRs labeled with B (i.e., B_1 and B_2) with the same decay rate κ_2 are the readout resonators and all the TLRs labeled with A with the decay rate κ_1 are the storage resonators. The circle with N stands for a superconducting molecule with the N -type level structure. The direction of the arrow represents the spread direction of the probe light. The elements labeled with a circular arrow in a big circle are circulators. $|\alpha\rangle$ represents the probe light. $|X\rangle\langle X|$ represents the homodyne measurement on the coherent state of the probe light.

B. The Quantum nondemolition measurement on total photon number of transmission-line resonators based on cross-Kerr effect

The total photon number of TLRs can be measured with QND by means of the cross-Kerr effect. The detailed schematic diagram is shown in Fig. 2. All the TLRs in the top and the bottom are the readout and storage resonators, respectively. The Homodyne detection has been used for microwave in circuit QED experiment [45]. The probe light in the coherent state $|\alpha\rangle$ is input from the left and measured via an X homodyne measurement on the right. Here, we use the input-output relationship to explain the whole process. When the probe light is resonant with readout resonators, the Heisenberg-Langevin equations for each cross-Kerr media in the probe light path are given by

$$\dot{\hat{b}}_k = -i\chi_k \hat{n}_k \hat{b}_k - \frac{\kappa_2}{2} \hat{b}_k - \sqrt{\kappa_2} \hat{b}_k^{in}, \quad (3)$$

where $k = 1, 2$ and $\hat{n}_k = \hat{a}_k^\dagger \hat{a}_k$ represents the photon number operator of the k -th storage resonator. We assume that all TLRs labeled with A and B have the same decay rates κ_1 and κ_2 , respectively.

Now, we consider the situation that the decay rate of the readout resonator $\kappa_2 \gg \chi_k \langle \hat{n}_k \rangle$. One can make $\dot{\hat{b}}_k = 0$ in Eq. (3). Combining with the standard cavity input-output relationship $\hat{b}_{out} = \hat{b}_{in} + \sqrt{\kappa_2} \hat{b}$ [65, 66], where \hat{b}_{in} and \hat{b}_{in}^\dagger satisfy the standard commutation relations $[\hat{b}_{in}(t), \hat{b}_{in}^\dagger(t')] = \delta(t - t')$, one can obtain the reflection coefficients which are expressed as

$$r_k(\hat{n}_k) = \frac{\hat{b}_k^{out}}{\hat{b}_k^{in}} = \frac{i\chi_k \hat{n}_k - \frac{\kappa_2}{2}}{i\chi_k \hat{n}_k + \frac{\kappa_2}{2}}. \quad (4)$$

Our goal is to make a QND measurement on the total photon number in two storage resonators (the two TLRs A_1 and A_2 in the bottom of Fig. 2). For this task, a probe light in the coherent state $|\alpha\rangle^{in}$ is input from the left, and let us assume that there are n_1 photons in TLR A_1 . When the probe light leaves TLR B_1 , the state of Kerr-1 becomes

$$|\psi\rangle_{K1}^{out} = |n_1\rangle |e^{i\theta_{n_1}} \alpha\rangle_1^{out}. \quad (5)$$

Here $\theta_{n_1} = \arg[r_1(n_1)]$ and $|n_1\rangle$ is a Fock state. One can make an X homodyne measurement to infer the photon number in TLR A_1 because the phase shift depends on the photon number n_1 . When the probe light passes through TLR B_2 , two Kerr media become a cascaded system. Therefore, we set $\hat{b}_2^{in} = \hat{b}_1^{out}$ because the input field of resonator B_2 is the output field of resonator B_1 . The input-output relationship of this cascaded system is $\hat{b}_2^{out} = r_2(n_2)r_1(n_1)\hat{b}_1^{in}$. Let us assume that the photon number in TLR A_2 is n_2 . After the probe light leaves resonator B_2 , its state is given by

$$|\alpha\rangle_2^{out} = |e^{i\theta_{n_1+n_2}} \alpha\rangle_2^{out}, \quad (6)$$

TABLE I: The corresponding relation between the states of the signal light and the phase shifts.

$ \hat{a}_1\rangle \otimes \hat{a}_2\rangle$	Total phase shift
$ 0\rangle \otimes 0\rangle$	$\arg[r_1(0) \cdot r_2(0)]$
$ 1\rangle \otimes 0\rangle$	$\arg[r_1(1) \cdot r_2(0)]$
$ 2\rangle \otimes 0\rangle$	$\arg[r_1(2) \cdot r_2(0)]$
$ 0\rangle \otimes 1\rangle$	$\arg[r_1(0) \cdot r_2(1)]$
$ 1\rangle \otimes 1\rangle$	$\arg[r_1(1) \cdot r_2(1)]$
$ 0\rangle \otimes 2\rangle$	$\arg[r_1(0) \cdot r_2(2)]$

where

$$\theta_{n_1+n_2} = \theta_{n_1} + \theta_{n_2} = \arg[r_1(n_1) \cdot r_2(n_2)], \quad (7)$$

where $\theta_{n_2} = \arg[r_2(n_2)]$.

To make an effective homodyne detection, we detect the position quadrature X of the coherent state. The wave function in the coherent state is given by [67, 68]

$$\langle X | \alpha e^{i\theta} \rangle = f(X, \alpha \cos \theta) e^{i\Phi(X)}, \quad (8)$$

where the functions are given by

$$f(X, y) = \frac{1}{\sqrt[4]{2\pi}} \exp\left[-\frac{1}{4}(x - 2y)^2\right]$$

$$\Phi(X) = \alpha \sin \theta (x - 2\alpha \cos \theta) \bmod(2\pi). \quad (9)$$

Therefore, for states $|\alpha e^{i\theta_1}\rangle$ and $|\alpha e^{i\theta_2}\rangle$, the midpoint and distance between the peaks of corresponding functions $f(X, \alpha \cos \theta_1)$ and $f(X, \alpha \cos \theta_2)$ are $X_m = \alpha(\cos \theta_1 + \cos \theta_2)$ and $X_d = 2\alpha(\cos \theta_1 - \cos \theta_2)$, respectively. According to the result of position, one can distinguish the different phases. The error probability is given by [68]

$$P_{\text{error}} = \frac{1}{2} \operatorname{erfc}\left[\frac{X_d}{2\sqrt{2}}\right], \quad (10)$$

where $\operatorname{erfc}(x)$ is the complementary error function.

When we only consider the maximal total photon number of two, all the different Fock states and corresponding phase shifts are shown in Table I.

III. ENTANGLEMENT PURIFICATION OF BIT-FLIPPING ERRORS FOR MICROWAVE PHOTONS

A. Entanglement purification protocol for microwave-photon pairs

Let us assume that the nonlocal microwave-photon pairs in quantum communication are in the mixed state $\hat{\rho}_{cd}$ described by

$$\hat{\rho}_{cd} = f |\Phi^\dagger\rangle_{cd} \langle \Phi^\dagger| + (1-f) |\Psi^\dagger\rangle_{cd} \langle \Psi^\dagger|, \quad (11)$$

TABLE II: The corresponding relation between the states of the signal light and the phase shifts by using the same cross-Kerr media in each QND detector.

$\hat{c}_1 \hat{c}_2 / \hat{d}_1 \hat{d}_2 (\hat{a}_1\rangle \hat{a}_2\rangle)$	Total phase shift
$ V\rangle V\rangle \rightarrow (0\rangle 1\rangle)$	θ_1
$ H\rangle H\rangle \rightarrow (1\rangle 0\rangle)$	θ_1
$ H\rangle V\rangle \rightarrow (1\rangle 1\rangle)$	θ_2
$ V\rangle H\rangle \rightarrow (0\rangle 0\rangle)$	θ_0

where

$$|\Phi^\dagger\rangle_{cd} = \frac{1}{\sqrt{2}} (|H\rangle_c |H\rangle_d + |V\rangle_c |V\rangle_d),$$

$$|\Psi^\dagger\rangle_{cd} = \frac{1}{\sqrt{2}} (|H\rangle_c |V\rangle_d + |V\rangle_c |H\rangle_d). \quad (12)$$

H and V represent the horizontal and the vertical polarizations of microwave photons, respectively. The symbol f with the relationship $f = \langle \Phi^\dagger | \hat{\rho}_{cd} | \Phi^\dagger \rangle$ is the fidelity of the state $|\Phi^\dagger\rangle$ ($f > \frac{1}{2}$). In this way, the state of the system composed of two microwave-photon pairs is just the mixture of four states. They are $|\Phi^\dagger\rangle_{c1d1} |\Phi^\dagger\rangle_{c2d2}$ with a probability of f^2 , $|\Phi^\dagger\rangle_{c1d1} |\Psi^\dagger\rangle_{c2d2}$ and $|\Psi^\dagger\rangle_{c1d1} |\Phi^\dagger\rangle_{c2d2}$ with the same probability of $(1-f)f$, and $|\Psi^\dagger\rangle_{c1d1} |\Psi^\dagger\rangle_{c2d2}$ with a probability of $(1-f)^2$.

The principle of our EPP for the polarization entanglement of nonlocal microwave-photon pairs from two identical ideal entanglement sources is shown in Fig. 3. Here, we choose two same cross-Kerr systems, i.e., $\chi_1 = \chi_2$, to accomplish the QND measurement process for parity check. We will discuss the physical implementation in Sec. III C. The microwave polarizing beam splitter (PBS) shown in Fig. 3 can pass the photons in the state $|H\rangle$ and reflect the photons in the state $|V\rangle$. Therefore, in the QND part of this protocol, we can change $|H\rangle$ and $|V\rangle$ to $|1\rangle$ and $|0\rangle$ for $\hat{c}_1 \hat{d}_1$, respectively. For $\hat{c}_2 \hat{d}_2$, $|H\rangle$ and $|V\rangle$ can be represented by $|0\rangle$ and $|1\rangle$, respectively. The different polarization states and corresponding phase shifts are rewritten in Table II. The two QND measurement detectors are identical and the two parties in quantum communication Alice and Bob hold \hat{c} and \hat{d} , respectively. We don't consider the phase difference of microwave photon after it leaves the storage resonator in our scheme, because we just design the principle here. The possible phase difference can be compensated in practice.

When the microwave-photon pairs in the state $|\Phi^\dagger\rangle_{c1d1} |\Phi^\dagger\rangle_{c2d2}$ pass through the parity-check QND detectors, the state of the composite system composed of the two microwave-photon pairs ($\hat{c}_1 \hat{d}_1$ and $\hat{c}_2 \hat{d}_2$) and the two probe lights (\hat{c} and \hat{d}) becomes

$$\begin{aligned} \Rightarrow & \frac{1}{2} \{ (|H\rangle_{c1} |H\rangle_{d1} |H\rangle_{c2} |H\rangle_{d2} \\ & + |V\rangle_{c1} |V\rangle_{d1} |V\rangle_{c2} |V\rangle_{d2}) |\alpha e^{i\theta_1}\rangle_c |\alpha e^{i\theta_1}\rangle_d \\ & + |H\rangle_{c1} |H\rangle_{d1} |V\rangle_{c2} |V\rangle_{d2} |\alpha e^{i\theta_2}\rangle_c |\alpha e^{i\theta_2}\rangle_d \end{aligned}$$

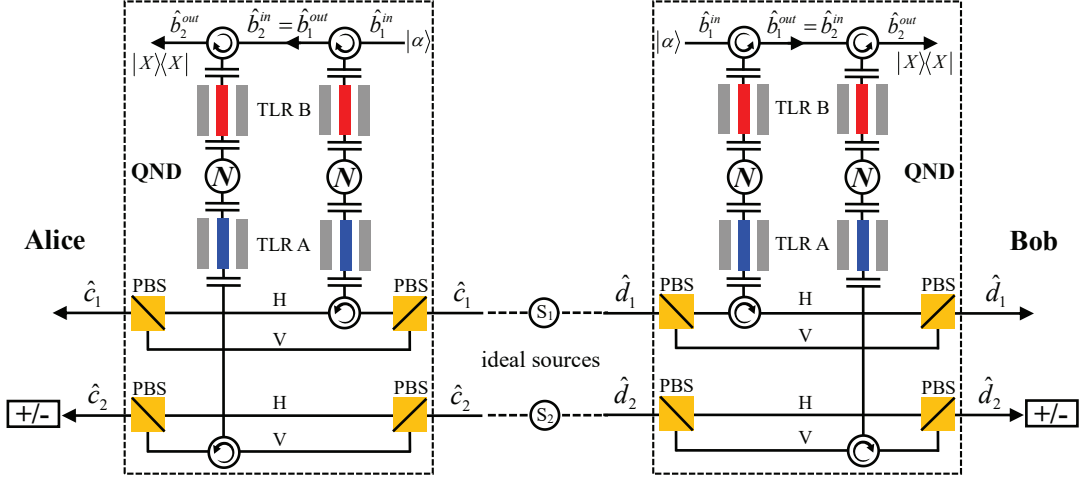


FIG. 3: Schematic diagram for the entanglement purification on two microwave-photon pairs. S_1 and S_2 are the two identical ideal entanglement sources for microwave-photon pairs. Two dashed boxes are two same-polarization parity-check QND detectors. PBS represents a polarizing beam splitter for microwave photons. The circles with a circular arrow stands for circulators. The QND measurement is given in Fig. 2. Two rectangular boxes labeled with $+/-$ signs are two measurements with the two diagonal bases $\{|\pm\rangle = \frac{1}{\sqrt{2}}(|H\rangle \pm |V\rangle)\}$.

$$+|V\rangle_{c1}|V\rangle_{d1}|H\rangle_{c2}|H\rangle_{d2}|\alpha e^{i\theta_0}\rangle_c|\alpha e^{i\theta_0}\rangle_d\}. \quad (13)$$

When Alice and Bob obtain a phase shift with θ_1 on their coherent states after the homodyne detections, the state will collapse to $(|H\rangle_{c1}|H\rangle_{d1}|H\rangle_{c2}|H\rangle_{d2} + |V\rangle_{c1}|V\rangle_{d1}|V\rangle_{c2}|V\rangle_{d2})$. For the last two terms, there are two situations. If $\theta_2 = \theta_0 + 2\pi$, the last two terms have the same phase shifts. At this point, both Alice and Bob obtain the phase shift θ_0 on their coherent states, the state becomes $(|H\rangle_{c1}|H\rangle_{d1}|V\rangle_{c2}|V\rangle_{d2} + |V\rangle_{c1}|V\rangle_{d1}|H\rangle_{c2}|H\rangle_{d2})$. Subsequently, Alice and Bob can perform a bit-flipping operation $\hat{\sigma}_x = |H\rangle\langle V| + |V\rangle\langle H|$ on \hat{c}_1 and \hat{d}_1 , respectively, and then they can obtain the state $(|H\rangle_{c1}|H\rangle_{d1}|H\rangle_{c2}|H\rangle_{d2} + |V\rangle_{c1}|V\rangle_{d1}|V\rangle_{c2}|V\rangle_{d2})$. If the $\theta_2 \neq \theta_0 + 2\pi$, Alice and Bob will obtain the different results, they will make no operation. To get the state $|\Phi^\dagger\rangle_{cd}$, Alice and Bob make a measurement with the diagonal basis $\{|\pm\rangle = \frac{1}{\sqrt{2}}(|H\rangle \pm |V\rangle)\}$ on \hat{c}_2 and \hat{d}_2 , respectively. When both their results are $|+\rangle$ or $|-\rangle$, the state of the microwave-photon pair $\hat{c}_1\hat{d}_1$ becomes $|\Phi^\dagger\rangle_{cd}$. Otherwise, they should make the operation $\hat{\sigma}_z = |H\rangle\langle H| - |V\rangle\langle V|$ on the microwave photon \hat{c}_1 to obtain the state $|\Phi^\dagger\rangle_{c1d1}$.

After the QND measurement process, the state of the system $|\Phi^\dagger\rangle_{c1d1}|\Psi^\dagger\rangle_{c2d2}|\alpha\rangle_c|\alpha\rangle_d$ becomes

$$\begin{aligned} \Rightarrow & \frac{1}{2}\{|H\rangle_{c1}|H\rangle_{d1}|V\rangle_{c2}|H\rangle_{d2}|\alpha e^{i\theta_2}\rangle_c|\alpha e^{i\theta_1}\rangle_d \\ & +|V\rangle_{c1}|V\rangle_{d1}|H\rangle_{c2}|V\rangle_{d2}|\alpha e^{i\theta_0}\rangle_c|\alpha e^{i\theta_1}\rangle_d \\ & +|H\rangle_{c1}|H\rangle_{d1}|H\rangle_{c2}|V\rangle_{d2}|\alpha e^{i\theta_1}\rangle_c|\alpha e^{i\theta_2}\rangle_d \\ & +|V\rangle_{c1}|V\rangle_{d1}|V\rangle_{c2}|H\rangle_{d2}|\alpha e^{i\theta_1}\rangle_c|\alpha e^{i\theta_0}\rangle_d\}. \quad (14) \end{aligned}$$

Another state $|\Psi^\dagger\rangle_{c1d1}|\Phi^\dagger\rangle_{c2d2}|\alpha\rangle_c|\alpha\rangle_d$ is evolved to

$$\begin{aligned} \Rightarrow & \frac{1}{2}\{|V\rangle_{c1}|H\rangle_{d1}|H\rangle_{c2}|H\rangle_{d2}|\alpha e^{i\theta_0}\rangle_c|\alpha e^{i\theta_1}\rangle_d \\ & +|H\rangle_{c1}|V\rangle_{d1}|V\rangle_{c2}|V\rangle_{d2}|\alpha e^{i\theta_2}\rangle_c|\alpha e^{i\theta_1}\rangle_d \\ & +|V\rangle_{c1}|H\rangle_{d1}|V\rangle_{c2}|V\rangle_{d2}|\alpha e^{i\theta_1}\rangle_c|\alpha e^{i\theta_2}\rangle_d \\ & +|H\rangle_{c1}|V\rangle_{d1}|H\rangle_{c2}|H\rangle_{d2}|\alpha e^{i\theta_1}\rangle_c|\alpha e^{i\theta_0}\rangle_d\}. \quad (15) \end{aligned}$$

From these two results, with the situation $\theta_2 = \theta_0 + 2\pi$, one can see that if Alice and Bob obtain the phase shifts θ_0 and θ_1 with a homodyne measurement on their probe lights \hat{c} and \hat{d} , the state of the two microwave-photon pairs $\hat{c}_1\hat{d}_1\hat{c}_2\hat{d}_2$ becomes $(|H\rangle_{c1}|H\rangle_{d1}|V\rangle_{c2}|H\rangle_{d2} + |V\rangle_{c1}|V\rangle_{d1}|H\rangle_{c2}|V\rangle_{d2})$ or $(|V\rangle_{c1}|H\rangle_{d1}|H\rangle_{c2}|H\rangle_{d2} + |H\rangle_{c1}|V\rangle_{d1}|V\rangle_{c2}|V\rangle_{d2})$. As Alice and Bob cannot determine on which pair a bit-flipping error occurs, they discard both photon pairs in these two situations. With the situation $\theta_2 \neq \theta_0 + 2\pi$, Alice and Bob get the different results for all the terms. They should also discard all these situations.

After the microwave-photon pairs pass through the QND detectors, the state of the system $|\Psi^\dagger\rangle_{c1d1}|\Psi^\dagger\rangle_{c2d2}|\alpha\rangle_c|\alpha\rangle_d$ turns to

$$\begin{aligned} \Rightarrow & \frac{1}{2}\{|V\rangle_{c1}|H\rangle_{d1}|V\rangle_{c2}|H\rangle_{d2} \\ & +|H\rangle_{c1}|V\rangle_{d1}|H\rangle_{c2}|V\rangle_{d2}|\alpha e^{i\theta_1}\rangle_c|\alpha e^{i\theta_1}\rangle_d \\ & +|V\rangle_{c1}|H\rangle_{d1}|H\rangle_{c2}|V\rangle_{d2}|\alpha e^{i\theta_0}\rangle_c|\alpha e^{i\theta_2}\rangle_d \\ & +|H\rangle_{c1}|V\rangle_{d1}|V\rangle_{c2}|H\rangle_{d2}|\alpha e^{i\theta_2}\rangle_c|\alpha e^{i\theta_0}\rangle_d\}. \quad (16) \end{aligned}$$

The result is similar to that in the situation with no bit-flipping error expressed in Eq. (13). Due to the indistinguishability with the situation with no bit-flipping

TABLE III: Corresponding relation between the states of the signal light in storage resonators and the phase shifts by choosing two same cross-Kerr systems in each QND detector.

State $ \hat{a}_1\rangle \hat{a}_2\rangle$	Total phase shift
$ 0\rangle 0\rangle$	θ_0
$ 1\rangle 0\rangle/ 0\rangle 1\rangle$	θ_1
$ 1\rangle 1\rangle$	θ_2
$ 2\rangle 0\rangle/ 0\rangle 2\rangle$	θ_3

errors, Alice and Bob should keep their photon pairs for the next round. That is, if Alice and Bob get the phase shift θ_1 , they obtain the state of the two photon pairs $(|V\rangle_{c1}|H\rangle_{d1}|V\rangle_{c2}|H\rangle_{d2} + |H\rangle_{c1}|V\rangle_{d1}|H\rangle_{c2}|V\rangle_{d2})$. If they both get the phase shift θ_0 (condition $\theta_2 = \theta_0 + 2\pi$), they get the state $(|V\rangle_{c1}|H\rangle_{d1}|H\rangle_{c2}|V\rangle_{d2} + |H\rangle_{c1}|V\rangle_{d1}|V\rangle_{c2}|H\rangle_{d2})$. Therefore, they make an operation $\hat{\sigma}_x = |V\rangle\langle H| + |H\rangle\langle V|$ on \hat{c}_2 and \hat{d}_2 to obtain the state $(|V\rangle_{c1}|H\rangle_{d1}|V\rangle_{c2}|H\rangle_{d2} + |H\rangle_{c1}|V\rangle_{d1}|H\rangle_{c2}|V\rangle_{d2})$. Subsequently, Alice and Bob make a measurement with the diagonal basis $\{|\pm\rangle = \frac{1}{\sqrt{2}}(|H\rangle \pm |V\rangle)\}$ on \hat{c}_2 and \hat{d}_2 . If they both obtain the results $|+\rangle$ or $|-\rangle$, the state of microwave-photon pairs $\hat{c}_1\hat{d}_1$ becomes $|\Psi^\dagger\rangle_{c_1d_1}$. Otherwise, they should make the operation $\hat{\sigma}_z = |H\rangle\langle H| - |V\rangle\langle V|$ on the microwave photon \hat{c}_1 to obtain the state $|\Psi^\dagger\rangle_{c_1d_1}$.

After the operations, Alice and Bob can obtain their nonlocal entangled state of microwave-photon pairs with more purity. In the ideal model, the fidelity of the remaining microwave-photon pairs is given by

$$f_{ideal} = \frac{f^2}{f^2 + (1-f)^2}. \quad (17)$$

B. Entanglement purification for polarization-spatial entangled microwave-photon pairs

The polarization-spatial entangled states are widely used in quantum communication as they can be produced by parametric down-conversion naturally in experiment. Therefore, considering the situation for polarization-spatial entangled microwave-photon pairs is very necessary. For a pair polarization-spatial entangled microwave photons, the state is given by $(\hat{c}_{1H}^\dagger\hat{d}_{1H}^\dagger + \hat{c}_{1V}^\dagger\hat{d}_{1V}^\dagger + \hat{c}_{2H}^\dagger\hat{d}_{2H}^\dagger + \hat{c}_{2V}^\dagger\hat{d}_{2V}^\dagger)|0\rangle$. Therefore, for the four-photon state, it can be described by $(\hat{c}_{1H}^\dagger\hat{d}_{1H}^\dagger + \hat{c}_{1V}^\dagger\hat{d}_{1V}^\dagger + \hat{c}_{2H}^\dagger\hat{d}_{2H}^\dagger + \hat{c}_{2V}^\dagger\hat{d}_{2V}^\dagger)^2|0\rangle$. The detailed schematic diagram of our EPP for those two situations is shown in Fig. 4. Here the states $|H\rangle$ and $|V\rangle$ are translated to $|1\rangle$ and $|0\rangle$ in $\hat{c}_1\hat{d}_1$ mode, respectively. In $\hat{c}_2\hat{d}_2$ mode, the corresponding relations are opposite. Here, we choose the two same cross-Kerr systems in each QND detector and the corresponding phase

shifts are given in Table III. We assume all the four angles are different in this section.

First, we consider the case where there is a pair of polarization-spatial entangled microwave photons. This time, it is just an ideal microwave-photon pair. After it passes through the QND detectors, the state composed of the microwave-photon pair and the probe light is given by

$$\begin{aligned} \implies & (\hat{c}_{1H}^\dagger\hat{d}_{1H}^\dagger + \hat{c}_{2V}^\dagger\hat{d}_{2V}^\dagger)|0\rangle|\alpha e^{i\theta_1}\rangle_c|\alpha e^{i\theta_1}\rangle_d \\ & + (\hat{c}_{1V}^\dagger\hat{d}_{1V}^\dagger + \hat{c}_{2H}^\dagger\hat{d}_{2H}^\dagger)|0\rangle|\alpha e^{i\theta_0}\rangle_c|\alpha e^{i\theta_0}\rangle_d. \end{aligned} \quad (18)$$

When Alice and Bob get the same phase shift θ_1 via an X homodyne measurement on their probe lights, they obtain the state of their microwave-photon pair $(\hat{c}_{1H}^\dagger\hat{d}_{1H}^\dagger + \hat{c}_{2V}^\dagger\hat{d}_{2V}^\dagger)|0\rangle$. After passing through the couplers, their photon pair will appear at the modes $\hat{c}_2\hat{d}_2$. When Alice and Bob get the same phase shift θ_0 , they obtain the state $(\hat{c}_{1V}^\dagger\hat{d}_{1V}^\dagger + \hat{c}_{2H}^\dagger\hat{d}_{2H}^\dagger)|0\rangle$, and then their photon pair will appear at the output modes $\hat{c}_1\hat{d}_1$. When the bit-flipping error occurs, the state becomes $(\hat{c}_{1V}^\dagger\hat{d}_{1H}^\dagger + \hat{c}_{2H}^\dagger\hat{d}_{2V}^\dagger + \hat{c}_{1H}^\dagger\hat{d}_{1V}^\dagger + \hat{c}_{2V}^\dagger\hat{d}_{2H}^\dagger)|0\rangle$. With the QND measurement, the state of the photon pair evolves to

$$\begin{aligned} \implies & (\hat{c}_{1V}^\dagger\hat{d}_{1H}^\dagger + \hat{c}_{2H}^\dagger\hat{d}_{2V}^\dagger)|0\rangle|\alpha e^{i\theta_0}\rangle_c|\alpha e^{i\theta_1}\rangle_d \\ & + (\hat{c}_{1H}^\dagger\hat{d}_{1V}^\dagger + \hat{c}_{2V}^\dagger\hat{d}_{2H}^\dagger)|0\rangle|\alpha e^{i\theta_1}\rangle_c|\alpha e^{i\theta_0}\rangle_d. \end{aligned} \quad (19)$$

Alice and Bob will get the different results θ_0 and θ_1 . They should perform a bit-flip operation of polarization $\hat{\sigma}_x = |V\rangle\langle H| + |H\rangle\langle V|$ on photon \hat{c}_1 to obtain the state $(\hat{c}_{1H}^\dagger\hat{d}_{1H}^\dagger + \hat{c}_{1V}^\dagger\hat{d}_{1V}^\dagger)|0\rangle$.

Second, we consider the case where there are two pairs of polarization-spatial entangled microwave photons. With no decoherence, the state of the two photon pairs is expressed as $(\hat{c}_{1H}^\dagger\hat{d}_{1H}^\dagger + \hat{c}_{1V}^\dagger\hat{d}_{1V}^\dagger + \hat{c}_{2H}^\dagger\hat{d}_{2H}^\dagger + \hat{c}_{2V}^\dagger\hat{d}_{2V}^\dagger)^2|0\rangle$. After the QND measurements are performed by Alice and Bob, the state of the whole system composed of the photon pair and the probe lights is

$$\begin{aligned} \implies & [(\hat{c}_{1H}^\dagger\hat{d}_{1H}^\dagger)^2 + (\hat{c}_{2V}^\dagger\hat{d}_{2V}^\dagger)^2]|0\rangle|\alpha e^{i\theta_3}\rangle_c|\alpha e^{i\theta_3}\rangle_d \\ & + 2\hat{c}_{1H}^\dagger\hat{d}_{1H}^\dagger\hat{c}_{2V}^\dagger\hat{d}_{2V}^\dagger|0\rangle|\alpha e^{i\theta_2}\rangle_c|\alpha e^{i\theta_2}\rangle_d \\ & + (\hat{c}_{1V}^\dagger\hat{d}_{1V}^\dagger + \hat{c}_{2H}^\dagger\hat{d}_{2H}^\dagger)^2|0\rangle|\alpha e^{i\theta_0}\rangle_c|\alpha e^{i\theta_0}\rangle_d \\ & + 2(\hat{c}_{1H}^\dagger\hat{d}_{1H}^\dagger + \hat{c}_{2V}^\dagger\hat{d}_{2V}^\dagger)(\hat{c}_{1V}^\dagger\hat{d}_{1V}^\dagger + \hat{c}_{2H}^\dagger\hat{d}_{2H}^\dagger) \\ & \otimes |0\rangle|\alpha e^{i\theta_1}\rangle_c|\alpha e^{i\theta_1}\rangle_d. \end{aligned} \quad (20)$$

Alice and Bob will get four results with θ_0 , θ_1 , θ_2 , and θ_3 which correspond to the states $(\hat{c}_{1V}^\dagger\hat{d}_{1V}^\dagger + \hat{c}_{2H}^\dagger\hat{d}_{2H}^\dagger)^2|0\rangle$, $(\hat{c}_{1H}^\dagger\hat{d}_{1H}^\dagger + \hat{c}_{2V}^\dagger\hat{d}_{2V}^\dagger)(\hat{c}_{1V}^\dagger\hat{d}_{1V}^\dagger + \hat{c}_{2H}^\dagger\hat{d}_{2H}^\dagger)|0\rangle$, $\hat{c}_{1H}^\dagger\hat{d}_{1H}^\dagger\hat{c}_{2V}^\dagger\hat{d}_{2V}^\dagger|0\rangle$, and $(\hat{c}_{1H}^\dagger\hat{d}_{1H}^\dagger)^2 + (\hat{c}_{2V}^\dagger\hat{d}_{2V}^\dagger)^2|0\rangle$, respectively. After the photons pass through the couplers, the states $[(\hat{c}_{1H}^\dagger\hat{d}_{1H}^\dagger)^2 + (\hat{c}_{2V}^\dagger\hat{d}_{2V}^\dagger)^2]|0\rangle$ and $(\hat{c}_{1V}^\dagger\hat{d}_{1V}^\dagger + \hat{c}_{2H}^\dagger\hat{d}_{2H}^\dagger)^2|0\rangle$ will appear at $\hat{c}_2\hat{d}_2$ and $\hat{c}_1\hat{d}_1$, respectively. The two photon pairs $(\hat{c}_{1H}^\dagger\hat{d}_{1H}^\dagger + \hat{c}_{2V}^\dagger\hat{d}_{2V}^\dagger)(\hat{c}_{1V}^\dagger\hat{d}_{1V}^\dagger + \hat{c}_{2H}^\dagger\hat{d}_{2H}^\dagger)|0\rangle$ will be divided into $\hat{c}_1\hat{d}_1$ and $\hat{c}_2\hat{d}_2$, respectively.

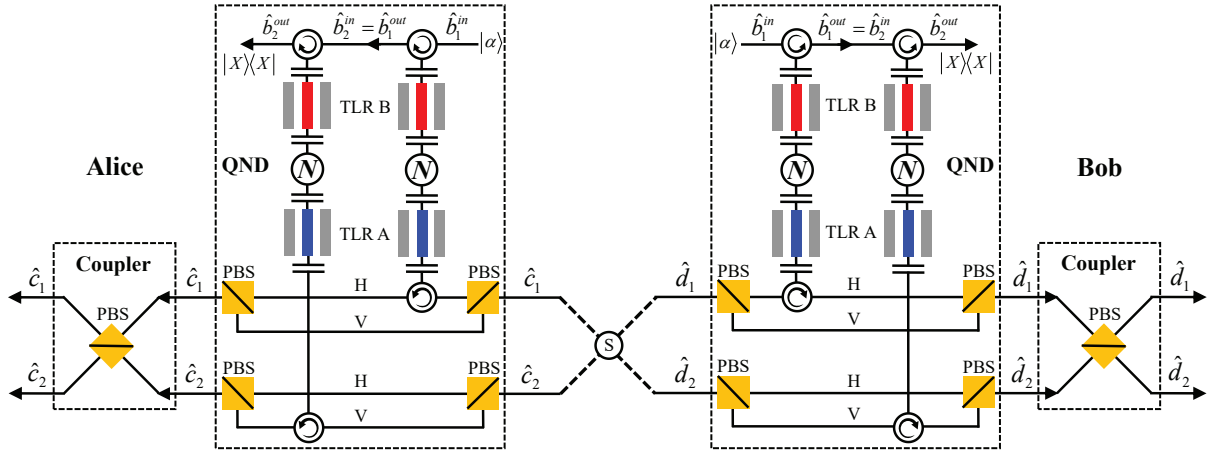


FIG. 4: Schematic diagram of our EPP for polarization-spatial entangled microwave-photon pairs. S is the entanglement source for generating polarization-spatial entangled microwave-photon pairs. The two big dashed boxes are two polarization parity-check QND detectors. The two small dashed boxes are two couplers with the same PBS for microwave photons.

When the bit-flipping error occurs, there will be two situations. The first situation is that only one of two microwave-photon pairs has an error, and the state of the two photon pairs becomes $(\hat{c}_{1H}^\dagger \hat{d}_{1H}^\dagger + \hat{c}_{1V}^\dagger \hat{d}_{1V}^\dagger + \hat{c}_{2H}^\dagger \hat{d}_{2H}^\dagger + \hat{c}_{2V}^\dagger \hat{d}_{2V}^\dagger)(\hat{c}_{1V}^\dagger \hat{d}_{1H}^\dagger + \hat{c}_{1H}^\dagger \hat{d}_{1V}^\dagger + \hat{c}_{2V}^\dagger \hat{d}_{2H}^\dagger + \hat{c}_{2H}^\dagger \hat{d}_{2V}^\dagger)|0\rangle$. Therefore, with the QND detector, the composite system composed of the two photon pairs and the two probe lights evolves to

$$\begin{aligned}
\Rightarrow & (\hat{c}_{1H}^\dagger \hat{d}_{1H}^\dagger \hat{c}_{1V}^\dagger \hat{d}_{1H}^\dagger + \hat{c}_{2V}^\dagger \hat{d}_{2V}^\dagger \hat{c}_{2H}^\dagger \hat{d}_{2V}^\dagger) \\
& \otimes |0\rangle |\alpha e^{i\theta_1}\rangle_c |\alpha e^{i\theta_3}\rangle_d \\
& + (\hat{c}_{1H}^\dagger \hat{d}_{1H}^\dagger \hat{c}_{2H}^\dagger \hat{d}_{2V}^\dagger + \hat{c}_{2V}^\dagger \hat{d}_{2V}^\dagger \hat{c}_{1V}^\dagger \hat{d}_{1H}^\dagger) \\
& \otimes |0\rangle |\alpha e^{i\theta_1}\rangle_c |\alpha e^{i\theta_2}\rangle_d \\
& + (\hat{c}_{1H}^\dagger \hat{d}_{1H}^\dagger \hat{c}_{1H}^\dagger \hat{d}_{1V}^\dagger + \hat{c}_{2V}^\dagger \hat{d}_{2V}^\dagger \hat{c}_{2V}^\dagger \hat{d}_{2H}^\dagger) \\
& \otimes |0\rangle |\alpha e^{i\theta_3}\rangle_c |\alpha e^{i\theta_1}\rangle_d \\
& + (\hat{c}_{1H}^\dagger \hat{d}_{1H}^\dagger \hat{c}_{2V}^\dagger \hat{d}_{2H}^\dagger + \hat{c}_{2V}^\dagger \hat{d}_{2V}^\dagger \hat{c}_{1H}^\dagger \hat{d}_{1V}^\dagger) \\
& \otimes |0\rangle |\alpha e^{i\theta_2}\rangle_c |\alpha e^{i\theta_1}\rangle_d \\
& + (\hat{c}_{1V}^\dagger \hat{d}_{1V}^\dagger + \hat{c}_{2H}^\dagger \hat{d}_{2H}^\dagger)(\hat{c}_{1V}^\dagger \hat{d}_{1H}^\dagger + \hat{c}_{2H}^\dagger \hat{d}_{2V}^\dagger) \\
& \otimes |0\rangle |\alpha e^{i\theta_0}\rangle_c |\alpha e^{i\theta_1}\rangle_d \\
& + (\hat{c}_{1V}^\dagger \hat{d}_{1V}^\dagger + \hat{c}_{2H}^\dagger \hat{d}_{2H}^\dagger)(\hat{c}_{1H}^\dagger \hat{d}_{1V}^\dagger + \hat{c}_{2V}^\dagger \hat{d}_{2H}^\dagger) \\
& \otimes |0\rangle |\alpha e^{i\theta_1}\rangle_c |\alpha e^{i\theta_0}\rangle_d
\end{aligned} \tag{21}$$

Analyzing from the result in Eq. (21), Alice and Bob know there exists an error in one pair when they get the different phase shifts. Alice and Bob should discard this result because they cannot get the state $(\hat{c}_{1H}^\dagger \hat{d}_{1H}^\dagger + \hat{c}_{2V}^\dagger \hat{d}_{2V}^\dagger)|0\rangle$ at $\hat{c}_1 \hat{d}_1$ and $\hat{c}_2 \hat{d}_2$.

The second one is the bit-flipping error taking place on both the two microwave photon pairs. The state becomes $(\hat{c}_{1V}^\dagger \hat{d}_{1H}^\dagger + \hat{c}_{1H}^\dagger \hat{d}_{1V}^\dagger + \hat{c}_{2V}^\dagger \hat{d}_{2H}^\dagger + \hat{c}_{2H}^\dagger \hat{d}_{2V}^\dagger)^2 |0\rangle$. When the two pairs pass the QND detectors, the state of the system will

evolve to

$$\begin{aligned}
\Rightarrow & [(\hat{c}_{1H}^\dagger \hat{d}_{1V}^\dagger)^2 + (\hat{c}_{2V}^\dagger \hat{d}_{2H}^\dagger)^2] |0\rangle |\alpha e^{i\theta_3}\rangle_c |\alpha e^{i\theta_0}\rangle_d \\
& + 2\hat{c}_{1H}^\dagger \hat{d}_{1V}^\dagger \hat{c}_{2V}^\dagger \hat{d}_{2H}^\dagger |0\rangle |\alpha e^{i\theta_2}\rangle_c |\alpha e^{i\theta_0}\rangle_d \\
& + [(\hat{c}_{1V}^\dagger \hat{d}_{1H}^\dagger)^2 + (\hat{c}_{2H}^\dagger \hat{d}_{2V}^\dagger)^2] |0\rangle |\alpha e^{i\theta_0}\rangle_c |\alpha e^{i\theta_3}\rangle_d \\
& + 2\hat{c}_{1V}^\dagger \hat{d}_{1H}^\dagger \hat{c}_{2H}^\dagger \hat{d}_{2V}^\dagger |0\rangle |\alpha e^{i\theta_0}\rangle_c |\alpha e^{i\theta_2}\rangle_d \\
& + 2(\hat{c}_{1V}^\dagger \hat{d}_{1H}^\dagger + \hat{c}_{2H}^\dagger \hat{d}_{2V}^\dagger)(\hat{c}_{1H}^\dagger \hat{d}_{1V}^\dagger + \hat{c}_{2V}^\dagger \hat{d}_{2H}^\dagger) \\
& \otimes |0\rangle |\alpha e^{i\theta_1}\rangle_c |\alpha e^{i\theta_1}\rangle_d.
\end{aligned} \tag{22}$$

Alice and Bob get the five results in which four results have different phase shifts and the other has the same phase shift. For the different phase shifts, they should discard the photon pairs because the pairs will appear in the same spatial mode. When Alice and Bob get the same phase shift, they cannot distinguish it from the situation with no error and they should keep the pairs. Then Alice and Bob can continue to purify the states by using the protocol presented for ideal entanglement sources discussed in Sec. III A.

C. Parameters and fidelity for quantum nondemolition detector

The cross-Kerr effect is induced by coupling two TLRs to a superconducting molecule as shown in Fig. 1. According to the previous works [19, 56], we choose the parameters of this superconducting system as $E_c/2\pi = 0.5$ GHz, $E_J/2\pi = 16$ GHz, and $E_m/2\pi = 0.2$ GHz. The two coupling strengths between the molecule and the TLRs are equal with $g_1/2\pi \sim g_2/2\pi \sim 300$ MHz. The classical pump field strength Ω_c and the detuning δ_2 are designed to $\Omega_c/2\pi \sim \delta_2/2\pi \sim 1.5$ GHz. Therefore, the cross-Kerr effect coefficient in our scheme is $|\chi|/2\pi \sim 2.4$ MHz. A recent experiment [59] demonstrated a state-dependent

shift $|\chi_{sc}|/2\pi = 2.59 \pm 0.06$ MHz between two cavities in circuit QED.

According to the parameters chosen above, we calculate the angle of the coherent state in Table III. The angles of states $|00\rangle$, $|10\rangle/|01\rangle$, $|11\rangle$ and $|20\rangle/|02\rangle$ are $\theta_0 = 0$, $\theta_1 \approx 0.6$, $\theta_2 \approx 1.2$ and $\theta_3 \approx 1.1$, respectively. Here, we choose the decay rate with $\kappa_2^{-1} \approx 10$ ns in our calculation. If we require that the minimal error probability is less than 0.01, according to the Eq. (10), then X_d should satisfy $X_d > 4.5$. Therefore, when the α satisfies $\alpha > 24.7$, all the angles can be distinguished. Here, the cross-Kerr effect is weak, the phase shifts in Table II can not satisfy the condition $\theta_2 = \theta_0 + 2\pi$. Therefore, in this physical system, Alice and Bob should make operations under the situation with different phase shifts.

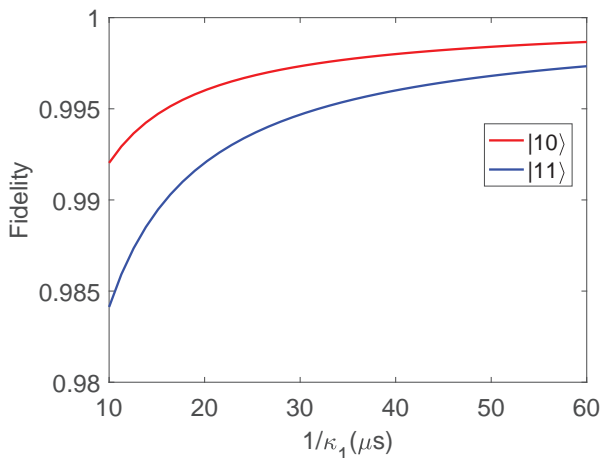


FIG. 5: The fidelity of the state in the storage resonators with dissipation for different decay rates κ_1^{-1} . Here the decay rate of the readout resonators is $\kappa_2^{-1} \sim 10$ ns.

In practice, the number of microwave photons will decrease due to the dissipation of storage resonators. The dynamics of the quantum system with dissipation is described by the master equation in Lindblad form given by

$$\frac{d\hat{\rho}(t)}{dt} = i[\hat{\rho}(t), \hat{H}] + \kappa_1 \hat{L}[\hat{a}_1] \hat{\rho}(t) + \kappa_1 \hat{L}[\hat{a}_2] \hat{\rho}(t), \quad (23)$$

where $\hat{\rho}(t)$ and \hat{H} are the density matrix and the Hamiltonian of the system, respectively. The symbols κ_1 represents the decay rates of TLR A. The superoperator \hat{L} with the rule $\hat{L}[\hat{\rho}] = (2\hat{\rho}\hat{\delta}^\dagger - \hat{\delta}^\dagger\hat{\rho} - \hat{\rho}\hat{\delta})/2$ represents the influence of the dissipation. Here, we assume that the QND measurement is ideal and that the probe light has no influence on the states in storage resonators. The fidelity is influenced by the leakage of the resonator. The formula of fidelity is $F = \langle \psi_{id} | \hat{\rho}(t) | \psi_{id} \rangle$, where the ideal state $|\psi_{id}\rangle$ is the initial state here. We consider the two initial states with $|10\rangle$ and $|11\rangle$. State $|nm\rangle$ represents n and m photons in storage resonator A_1 and A_2 , respectively. We calculate the fidelities of the states in storage

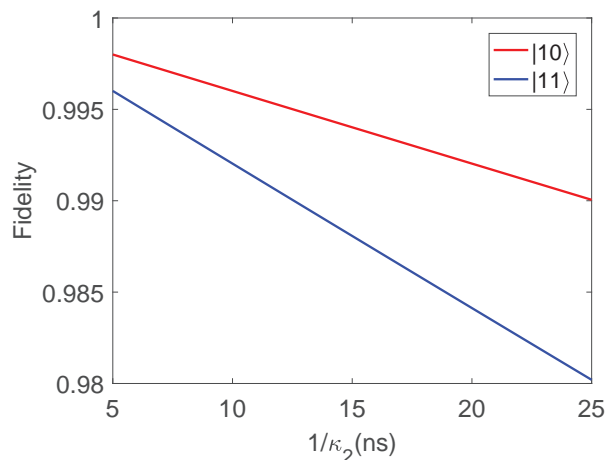


FIG. 6: The fidelity of the state in the storage resonators with dissipation for different decay rates of the readout resonators κ_2^{-1} . Here the decay rate of the storage resonators is $\kappa_1^{-1} \sim 20$ μ s.

resonators at the end of the measuring time. In the rotating frame, the Hamiltonian of the resonator is zero. We choose the total measuring time of the cascade system with $\tau \sim 8/\kappa_2$. The decay rate of the readout resonator keeps $\kappa_2^{-1} \sim 10$ ns in the whole process. The fidelities are proportional to κ_1^{-1} in Fig. 5, which indicates that the large storage time (the better resonator) can protect the microwave photons from dissipation. Then we plot the influences from the different κ_2 in Fig. 6. The parameter here is $\kappa_1^{-1} \sim 20$ μ s. Contrary to Fig. 5, the fidelities are inversely proportional to κ_2^{-1} in Fig. 6. The large κ_2^{-1} means a long measuring time. Therefore, as κ_2^{-1} becomes large, it will result in more total dissipation and the fidelity becomes lower.

IV. SUMMARY

In summary, we have proposed a physically feasible polarization EPP for the entangled state of nonlocal microwave photons in circuit QED. Our EPP includes two processes. The first process is used to purify the polarization entanglement state generated by the ideal entanglement sources and the second process is used for polarization-spatial entangled microwave-photon pairs. In our EPP, we design the polarization parity-check QND detectors to realize the postselection of microwave-photon quantum states. According to the phase shifts of the probe light hold by the two remote parties in quantum communication, say Alice and Bob, the parties can distinguish whether the error takes place and then correct it. We implement the QND measurement based on the cross-Kerr effect induced by coupling the two TLRs to a superconducting molecule. Our work can improve the practical application of microwave-based quantum

communication. For example, quantum repeaters are the indispensable parts in long-distance quantum communication. Due to the unavoidable influence of the environment in the processes of transmission and storage, the nonlocal near maximally entangled state generated between every two neighboring nodes and used as the quantum channel in a quantum repeater may turn into a mixed entangled state. Therefore, our purification protocol can be used here. Also, in the actual situation of satellite quantum communication, when the microwave signals pass through the aerosphere from the quantum satellite to the ground, the pure maximally entangled microwave-photon state may become the mixed one due to the influence of environment in the process of satellite quantum communication. To keep the communication efficient, the parties can use our EPP to purify the mixed

entangled microwave-photon state to improve its fidelity.

ACKNOWLEDGMENTS

We thank Guan-Yu Wang, Jing Qiu, and Zhi-Sheng Yang for helpful discussions. This work is supported by the National Natural Science Foundation of China under Grants No. 11674033, No. 11474026, and No. 11474027, the Fundamental Research Funds for the Central Universities under Grant No. 2015KJJC01, and the National Key Basic Research Program of China under Grant No. 2013CB922000.

-
- [1] C. H. Bennett, G. Brassard, C. Crepeau, R. Jozsa, A. Peres, and W. K. Wootters, Teleporting an Unknown Quantum State via Dual Classical and Einstein-Podolsky-Rosen Channels, *Phys. Rev. Lett.* **70**, 1895 (1993).
- [2] C. H. Bennett and S. J. Wiesner, Communication via One- and Two-Particle Operators on Einstein-Podolsky-Rosen states, *Phys. Rev. Lett.* **69**, 2881 (1992).
- [3] X. S. Liu, G. L. Long, D. M. Tong, and F. Li, General scheme for superdense coding between multiparties, *Phys. Rev. A* **65**, 022304 (2002).
- [4] A. K. Ekert, Quantum Cryptography Based on Bell's Theorem, *Phys. Rev. Lett.* **67**, 661 (1991).
- [5] C. H. Bennett, G. Brassard, and N. D. Mermin, Quantum Cryptography Without Bell's Theorem, *Phys. Rev. Lett.* **68**, 557 (1992).
- [6] X. H. Li, F. G. Deng, and H. Y. Zhou, Efficient quantum key distribution over a collective noise channel, *Phys. Rev. A* **78**, 022321 (2008).
- [7] M. Hillery, V. Bužek, and A. Berthiaume, Quantum secret sharing, *Phys. Rev. A* **59**, 1829 (1999).
- [8] G. L. Long and X. S. Liu, Theoretically efficient high-capacity quantum-key-distribution scheme, *Phys. Rev. A* **65**, 032302 (2002).
- [9] F. G. Deng, G. L. Long, and X. S. Liu, Two-step quantum direct communication protocol using the Einstein-Podolsky-Rosen pair block, *Phys. Rev. A* **68**, 042317 (2003).
- [10] C. Wang, F. G. Deng, Y. S. Li, X. S. Liu, and G. L. Long, Quantum secure direct communication with high-dimension quantum superdense coding, *Phys. Rev. A* **71**, 044305 (2005).
- [11] W. Zhang, D. S. Ding, Y. B. Sheng, L. Zhou, B. S. Shi, and G. C. Guo, Quantum secure direct communication with quantum memory, *Phys. Rev. Lett.* **118**, 220501 (2017).
- [12] Z. D. Walton, A. F. Abouraddy, A. V. Sergienko, B. E. A. Saleh, and M. C. Teich, Decoherence-Free Subspaces in Quantum Key Distribution, *Phys. Rev. Lett.* **91**, 087901 (2003).
- [13] J. C. Boileau, D. Gottesman, R. Laflamme, D. Poulin, and R. W. Spekkens, Robust Polarization-Based Quantum Key Distribution Over a Collective-Noise Channel, *Phys. Rev. Lett.* **92**, 017901 (2004).
- [14] J. C. Boileau, R. Laflamme, M. Laforest, and C. R. Myers, Robust Quantum Communication Using a Polarization-Entangled Photon Pair, *Phys. Rev. Lett.* **93**, 220501 (2004).
- [15] C. H. Bennett, H. J. Bernstein, S. Popescu, and B. Schumacher, Concentrating partial entanglement by local operations, *Phys. Rev. A* **53**, 2046 (1996).
- [16] Y. B. Sheng, F. G. Deng, and H. Y. Zhou, Nonlocal entanglement concentration scheme for partially entangled multipartite systems with nonlinear optics, *Phys. Rev. A* **77**, 062325 (2008).
- [17] B. C. Ren, F. F. Du, and F. G. Deng, Hyperentanglement concentration for two-photon four-qubit systems with linear optics, *Phys. Rev. A* **88**, 012302 (2013).
- [18] X. H. Li and S. Ghose, Hyperentanglement concentration for time-bin and polarization hyperentangled photons, *Phys. Rev. A* **91**, 062302 (2015).
- [19] H. Zhang and H. Wang, Entanglement concentration of microwave photons based on the Kerr effect in circuit QED, *Phys. Rev. A* **95**, 052314 (2017).
- [20] C. H. Bennett, G. Brassard, S. Popescu, B. Schumacher, J. A. Smolin, and W. K. Wootters, Purification of Noise Entanglement and Faithful Teleportation via Noisy Channels, *Phys. Rev. Lett.* **76**, 722 (1996).
- [21] D. Deutsch, A. Ekert, R. Jozsa, C. Macchiavello, S. Popescu, and A. Sanpera, Quantum Privacy Amplification and the Security of Quantum Cryptography over Noisy Channels, *Phys. Rev. Lett.* **77**, 2818 (1996).
- [22] J. W. Pan, C. Simon, C. Brukner, and A. Zeilinger, Entanglement purification for quantum communication, *Nature (London)* **410**, 1067 (2001).
- [23] C. Simon and J.W. Pan, Polarization Entanglement Purification using Spatial Entanglement, *Phys. Rev. Lett.* **89**, 257901 (2002).
- [24] J. W. Pan, S. Gasparoni, R. Ursin, G. Weihs, and A. Zeilinger, Experimental entanglement purification of arbitrary unknown states, *Nature (London)* **423**, 417 (2003).
- [25] Y. B. Sheng, F. G. Deng, and H. Y. Zhou, Efficient polarization-entanglement purification based on para-

- metric down-conversion sources with cross-Kerr nonlinearity, *Phys. Rev. A* **77**, 042308 (2008).
- [26] Y. B. Sheng and F. G. Deng, Deterministic entanglement purification and complete nonlocal Bell-state analysis with hyperentanglement, *Phys. Rev. A* **81**, 032307 (2010).
- [27] Y. B. Sheng and F. G. Deng, One-step deterministic polarization-entanglement purification using spatial entanglement, *Phys. Rev. A* **82**, 044305 (2010).
- [28] X. H. Li, Deterministic polarization-entanglement purification using spatial entanglement, *Phys. Rev. A* **82**, 044304 (2010).
- [29] F. G. Deng, One-step error correction for multipartite polarization entanglement, *Phys. Rev. A* **83**, 062316 (2011).
- [30] B. C. Ren, F. F. Du, and F. G. Deng, Two-step hyperentanglement purification with the quantum-state-joining method, *Phys. Rev. A* **90**, 052309 (2014).
- [31] G. Y. Wang, Q. Liu, and F. G. Deng, Hyperentanglement purification for two-photon six-qubit quantum systems, *Phys. Rev. A* **94**, 032319 (2016).
- [32] C. Wang, Y. Zhang, and G. S. Jin, Entanglement purification and concentration of electron-spin entangled states using quantum-dot spins in optical microcavities, *Phys. Rev. A* **84**, 032307 (2011).
- [33] Y. B. Sheng and L. Zhou, Deterministic polarization entanglement purification using time-bin entanglement, *Laser Phys. Lett.* **11**, 085203 (2014).
- [34] Y. B. Sheng and L. Zhou, Deterministic entanglement distillation for secure double-server blind quantum computation, *Sci. Rep.* **5**, 7815 (2015).
- [35] R. F. Werner, Quantum states with Einstein-Podolsky-Rosen correlations admitting a hidden-variable model, *Phys. Rev. A* **40**, 4277 (1989).
- [36] A. Blais, R. S. Huang, A. Wallraff, S. M. Girvin, and R. J. Schoelkopf, Cavity quantum electrodynamics for superconducting electrical circuits: An architecture for quantum computation, *Phys. Rev. A* **69**, 062320 (2004).
- [37] A. Wallraff, D. I. Schuster, A. Blais, L. Frunzio, R. S. Huang, J. Majer, S. Kumar, S. M. Girvin, and R. J. Schoelkopf, Strong coupling of a single photon to a superconducting qubit using circuit quantum electrodynamics, *Nature (London)* **431**, 162 (2004).
- [38] A. Blais, J. Gambetta, A. Wallraff, D. I. Schuster, S. M. Girvin, M. H. Devoret, and R. J. Schoelkopf, Quantum information processing with circuit quantum electrodynamics, *Phys. Rev. A* **75**, 032329 (2007).
- [39] L. DiCarlo, J. M. Chow, J. M. Gambetta, Lev S. Bishop, B. R. Johnson, D. I. Schuster, J. Majer, A. Blais, L. Frunzio, S. M. Girvin, and R. J. Schoelkopf, Demonstration of two-qubit algorithms with a superconducting quantum processor, *Nature (London)* **460**, 240 (2009).
- [40] Y. Cao, W. Y. Huo, Q. Ai, and G. L. Long, Theory of degenerate three-wave mixing using circuit QED in solid-state circuits, *Phys. Rev. A* **84**, 053846 (2011).
- [41] H. Wang, M. Mariantoni, R. C. Bialczak, M. Lenander, E. Lucero, M. Neeley, A. D. O'Connell, D. Sank, M. Weides, J. Wenner, T. Yamamoto, Y. Yin, J. Zhao, J. M. Martinis, and A. N. Cleland, Deterministic entanglement of photons in two superconducting microwave resonators, *Phys. Rev. Lett.* **106**, 060401 (2011).
- [42] Y. Hu and L. Tian, Deterministic generation of entangled photons in superconducting resonator arrays, *Phys. Rev. Lett.* **106**, 257002 (2011).
- [43] A. Fedorov, L. Steffen, M. Baur, M. P. da Silva, and A. Wallraff, Implementation of a Toffoli gate with superconducting circuits, *Nature (London)* **481**, 170 (2012).
- [44] M. D. Reed, L. DiCarlo, S. E. Nigg, L. Sun, L. Frunzio, S. M. Girvin, and R. J. Schoelkopf, Realization of three-qubit quantum error correction with superconducting circuits, *Nature (London)* **482**, 382 (2012).
- [45] R. Vijay, C. Macklin, D. H. Slichter, S. J. Weber, K. W. Murch, R. Naik, A. N. Korotkov, and I. Siddiqi, Stabilizing Rabi oscillations in a superconducting qubit using quantum feedback, *Nature (London)* **490**, 77 (2012).
- [46] F. W. Strauch, All-resonant control of superconducting resonators, *Phys. Rev. Lett.* **109**, 210501 (2012).
- [47] D. I. Schuster, A. A. Houck, J. A. Schreier, A. Wallraff, J. M. Gambetta, A. Blais, L. Frunzio, J. Majer, B. Johnson, M. H. Devoret, S. M. Girvin, and R. J. Schoelkopf, Resolving photon number states in a superconducting circuit, *Nature (London)* **445**, 515 (2007).
- [48] A. A. Houck, D. I. Schuster, J. Gambetta, J. A. Schreier, B. R. Johnson, J. M. Chow, L. Frunzio, J. Majer, M. H. Devoret, S. M. Girvin, and R. J. Schoelkopf, Generating single microwave photons in a circuit, *Nature (London)* **449**, 328 (2007).
- [49] J. Majer, J. M. Chow, J. M. Gambetta, J. Koch, B. R. Johnson, J. A. Schreier, L. Frunzio, D. I. Schuster, A. A. Houck, A. Wallraff, A. Blais, M. H. Devoret, S. M. Girvin, and R. J. Schoelkopf, Coupling superconducting qubits via a cavity bus, *Nature (London)* **449**, 443 (2007).
- [50] M. Hofheinz, E. M. Weig, M. Ansmann, R. C. Bialczak, E. Lucero, M. Neeley, A. D. O'Connell, H. Wang, J. M. Martinis, and A. N. Cleland, Generation of Fock states in a superconducting quantum circuit, *Nature (London)* **454**, 310 (2008).
- [51] B. R. Johnson, M. D. Reed, A. A. Houck, D. I. Schuster, Lev S. Bishop, E. Ginossar, J. M. Gambetta, L. DiCarlo, L. Frunzio, S. M. Girvin and R. J. Schoelkopf, Quantum non-demolition detection of single microwave photons in a circuit, *Nat. Phys.* **6**, 663 (2010).
- [52] M. Hua, M. J. Tao, and F. G. Deng, Universal quantum gates on microwave photons assisted by circuit quantum electrodynamics, *Phys. Rev. A* **90**, 012328 (2014).
- [53] A. Narla, S. Shankar, M. Hatridge, Z. Leghtas, K. M. Sliwa, E. Zalys-Geller, S. O. Mundhada, W. Pfaff, L. Frunzio, R. J. Schoelkopf, and M. H. Devoret, Robust Concurrent Remote Entanglement Between Two Superconducting Qubits, *Phys. Rev. X* **6**, 031036 (2016).
- [54] S. Rebić, J. Twamley, and G. J. Milburn, Giant Kerr nonlinearities in circuit quantum electrodynamics, *Phys. Rev. Lett.* **103**, 150503 (2009).
- [55] S. Kumar and D. P. DiVincenzo, Exploiting Kerr cross nonlinearity in circuit quantum electrodynamics for non-demolition measurements, *Phys. Rev. B* **82**, 014512 (2010).
- [56] Y. Hu, G. Q. Ge, S. Chen, X. F. Yang, and Y. L. Chen, Cross-Kerr-effect induced by coupled Josephson qubits in circuit quantum electrodynamics, *Phys. Rev. A* **84**, 012329 (2011).
- [57] G. Kirchmair, B. Vlastakis, Z. Leghtas, S. E. Nigg, H. Paik, E. Ginossar, M. Mirrahimi, L. Frunzio, S. M. Girvin, and R. J. Schoelkopf, Observation of quantum state collapse and revival due to the single-photon Kerr effect, *Nature (London)* **495**, 205 (2013).
- [58] I. C. Hoi, A. F. Kockum, T. Palomaki, T. M. Stace, B. Fan, L. Tornberg, S. R. Sathyamoorthy, G. Johansson, P. Delsing, and C. M. Wilson, Giant cross-Kerr effect for

- propagating microwaves induced by an artificial atom, *Phys. Rev. Lett.* **111**, 053601 (2013).
- [59] E. T. Holland, B. Vlastakis, R. W. Heeres, M. J. Reagor, U. Vool, Z. Leghtas, L. Frunzio, G. Kirchmair, M. H. Devoret, M. Mirrahimi and R. J. Schoelkopf, Single-photon-resolved cross-Kerr interaction for autonomous stabilization of photon-number states, *Phys. Rev. Lett.* **115**, 180501 (2015).
- [60] J. M. Hao, Y. Yuan, L. X. Ran, T. Jiang, J. A. Kong, C. T. Chan, and L. Zhou, Manipulating electromagnetic wave polarizations by anisotropic metamaterials, *Phys. Rev. Lett.* **99**, 063908 (2007).
- [61] D. R. Solli, C. F. McCormick, R. Y. Chiao, and J. M. Hickmann, Photonic crystal polarizers and polarizing beam splitters, *J. Appl. Phys.* **93**, 9429 (2003).
- [62] J. Koch, T. M. Yu, J. M. Gambetta, A. A. Houck, D. I. Schuster, J. Majer, A. Blais, M. H. Devoret, S. M. Girvin, and R. J. Schoelkopf, Charge-insensitive qubit design derived from the Cooper pair box, *Phys. Rev. A* **76**, 042319 (2007).
- [63] J. Siewert, R. Fazio, G. M. Palma, and E. Sciacca, Aspects of qubit dynamics in the presence of leakage, *J. Low Temp. Phys.* **118**, 795 (2000).
- [64] A. Imamoglu, H. Schmidt, G. Woods, and M. Deutsch, Strongly Interacting Photons in a Nonlinear Cavity, *Phys. Rev. Lett.* **79**, 1467 (1997).
- [65] D. F. Walls and G. J. Milburn, *Quantum Optics* (Springer-Verlag, Berlin, 1994).
- [66] K. Lalumière, B. C. Sanders, A. F. van Loo, A. Fedorov, A. Wallraff, and A. Blais, Input-output theory for waveguide QED with an ensemble of inhomogeneous atoms, *Phys. Rev. A* **88**, 043806 (2013).
- [67] K. Nemoto and W. J. Munro, Nearly Deterministic Linear Optical Controlled-NOT Gate, *Phys. Rev. Lett.* **93**, 250502 (2004).
- [68] S. D. Barrett, P. Kok, K. Nemoto, R. G. Beausoleil, W. J. Munro, and T. P. Spiller, Symmetry analyzer for nondestructive Bell-state detection using weak nonlinearities, *Phys. Rev. A* **71**, 060302(R) (2005).